


cambridge.org/mrf

G. Bulla¹, A. A. de Salles¹ and C. Fernández-Rodríguez² 

¹Electrical Engineering Department, UFRGS-Federal University of Rio Grande do Sul, P. Alegre, RS, Brazil and ²IFRS, Federal Institute for Education, Science and Technology of Rio Grande do Sul, Canoas, RS, Brazil

Research Paper

Cite this article: Bulla G, de Salles AA, Fernández-Rodríguez C (2020). Novel monopole antenna on a single AMC cell for low SAR. *International Journal of Microwave and Wireless Technologies* **12**, 825–830. <https://doi.org/10.1017/S1759078720000458>

Received: 30 November 2019

Revised: 3 April 2020

Accepted: 6 April 2020

First published online: 28 April 2020

Keywords:

Specific absorption rate; SAR reduction; artificial magnetic conductor; printed antennas

Author for correspondence:

C. Fernández-Rodríguez, E-mail: claudio.fernandez@canoas.ifrs.edu.br

Abstract

The design, simulations, and optimized results for a novel low specific absorption rate (SAR) monopole antenna on a single artificial magnetic conductor (AMC) cell are described in this paper. Simulated results show a reduction close to 70% in the 1 g ps SAR for the developed monopole antenna with the AMC in comparison to the monopole antenna without AMC. This allows higher radiation efficiency, battery drain reduction as well as mobile terminal user health risks reduction.

Introduction

Conventional antennas now used in wireless devices such as mobile phones, smartphones, tablets, and laptops are monopole, helix, or planar antennas without back plane. These antennas show a far-field radiation pattern close to isotropic or omnidirectional. In these antennas, the energy radiated against the mobile device users can be elevated and the specific absorption rate (SAR, which is defined as the power absorbed by a unit mass of body tissue) in their head or body tissues is therefore expected to be high. Computer simulations (e.g. based on the finite-difference time-domain method) confirm electromagnetic (EM) field penetration and high SAR in shallow and deeper structures in the brain [1–3].

Tests carried out by the French National Frequencies Agency (ANFR) between 2012 and 2016 on several hundred mobile phones show that the SARs are well above European regulatory limits (ICNIRP = 2 W/kg, on 10 g of tissue) [4], some of which may exceed the authorized thresholds by nearly four times, and even more if we refer to the American standards (IEEE/FCC = 1.6 W/kg, on 1 g of tissue) [5, 6], some smartphones exceeding 25 W/kg. They measured SARs with separation distances recommended by individual manufacturers as well as placements that were closer at 5 and 0 m to mimic actual use conditions by consumers holding the wireless device against the body and head [7].

Since mobile phones are usually operated in close proximity to the human head and many users stay long periods of time in their calls, the short- and long-term biological effects of the EM energy radiated from the cell phone antennas have attracted significant interest to the research community. Epidemiologic studies from some nations where mobile phone use has been extensive for a decade or longer indicate significantly increased risk of a variety of brain tumors, such as glioma and parotid gland tumors [8–11].

In 2011, the International Agency for Cancer Research (IARC; which is part of the World Health Organization (WHO)) classified these radiations as “possible carcinogenic for humans” (Group 2B). In addition, the WHO recommended the adoption of the “ALARA Principle” – As Low As Reasonably Achievable [12, 13].

Therefore, SAR reduction is a goal of growing interest. Various techniques have been discussed in the last decades to reduce the mobile terminal’s SAR, especially developing techniques for the reduction of the interaction between the mobile device antenna and the user’s head and body aiming to reduce the SAR while reducing degradations of the relevant antenna characteristics (such as input impedance, bandwidth, efficiency, as well as the moderate increase of the antenna’s front-to-back ratio) were investigated by some authors [14–25].

This could be reached by interposing electric conducting strips [15] or surfaces [16] between the antenna and the user. This also could be attained using magnetic conducting surfaces [17, 18] and other planar or mushroom-like metamaterials [19]. Additionally, this should result in more stable antenna characteristics decreasing dependence on the presence and proximity of the user [20]. SAR reductions in the range of 25–75% were achieved while improving or preserving good performance by several authors [21–25].

A novel low SAR monopole antenna design using a single artificial magnetic conductor (AMC) cell is described in this paper. The aim of this antenna is to reduce the energy absorbed in the mobile device user’s head including a single AMC cell and a conductive back plane between the monopole and the user’s head, with the aim to concentrate the EM field to the semi-space opposite to the user and hence reduce the energy radiated against the user, thanks

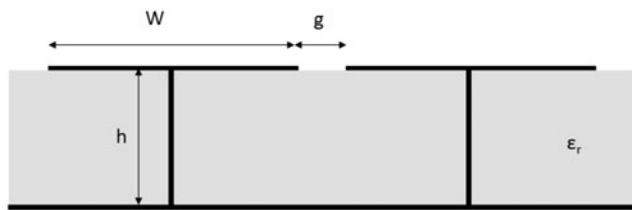


Fig. 1. Mushroom-like AMC structure.

to the screening effect of the AMC and the backplane. Hence, a moderate front-to-back ratio on their far-field radiation pattern can be achieved and therefore the SAR in the mobile device user’s head and body is expected to be reduced. One antenna on AMC cell is designed to resonate at 900 MHz and other at 1900 MHz.

AMC design and simulation

For a mushroom-type AMC structure, shown in Fig. 1, the surface sheet impedance is usually assigned equal to the impedance of a parallel LC resonant circuit [26]

$$Z_s = \frac{j\omega L}{1 - \omega^2 LC} \tag{1}$$

The resonance frequency is given by

$$f_0 = \frac{1}{2\pi\sqrt{LC}} \tag{2}$$

The impedance is inductive at low frequencies and capacitive at higher frequencies. At the resonance frequency, the impedance is theoretically infinite.

The high impedance ensures that a plane wave will be reflected without phase reversal.

For this type of structure, the capacitance is given by

$$C = \frac{W\epsilon_0(1 + \epsilon_r)}{\pi} \cosh^{-1}\left(\frac{W + g}{g}\right) \tag{3}$$

and the inductance

$$L = \mu h. \tag{4}$$

The AMC cell used in this work includes two patches on the top side, a full back plane and two side shorting planes, as shown in Fig. 2. Three layers of Rogers RT/Duroid 5880 are

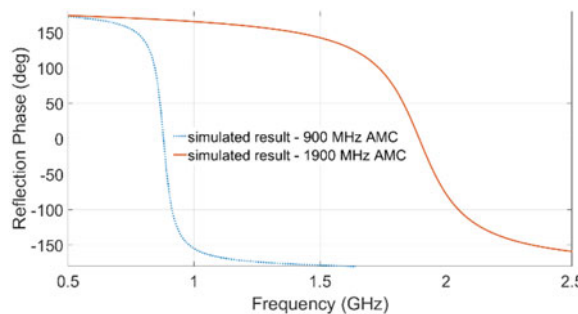


Fig. 3. Simulated reflection phase for a normally incident plane wave on the AMC structure.

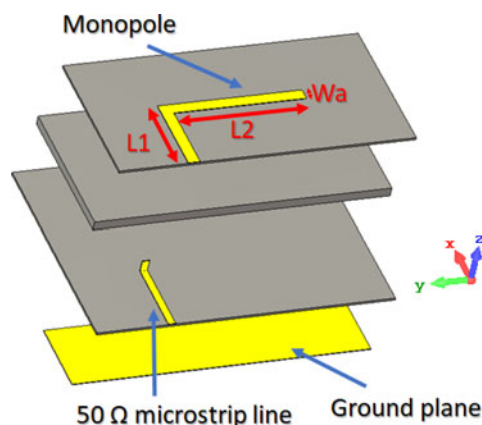


Fig. 4. Exploded view of the quarter wavelength monopole.

used to design the AMC. The dimensions are parametrically analyzed to have 0° phase reflection at 900 or 1900 MHz. The CST Studio® software was employed to determine the reflection phase for a normally incident plane wave on the AMC structure.

The simulated reflection phase is shown in Fig. 3 for the following set of parameters: $h_1 = h_3 = 0.8$ mm, $h_2 = 3.175$ mm, $S = 2$ mm, $S_x = 1$ mm, $S_y = 0$ mm, $L = 100$ mm, $W = 50$ mm for the AMC with 0° phase reflection at 900 MHz, and $h_1 = h_3 = 0.8$ mm, $h_2 = 3.175$ mm, $S = 2$ mm, $S_x = 1$ mm, $S_y = 0$ mm, $L = 40$ mm, $W = 20$ mm for the AMC with 0° phase reflection at 1900 MHz.

Design of a monopole on AMC for low SAR

Two quarter wavelength bent printed monopoles are designed, one to resonate at 900 MHz and other to resonate at 1900 MHz. The monopole antennas layout in exploded view is shown in

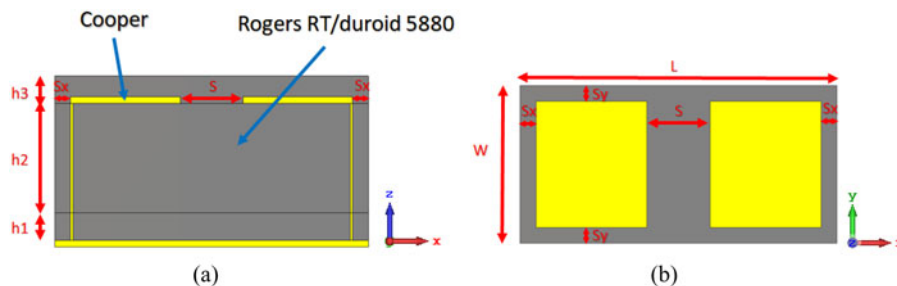


Fig. 2. The AMC cell layout.

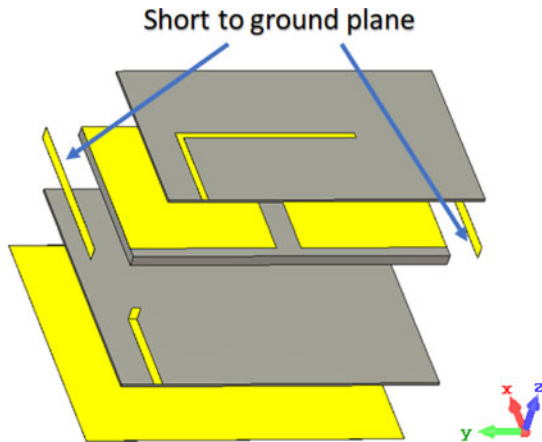


Fig. 5. Exploded view of the monopole on the AMC cell.

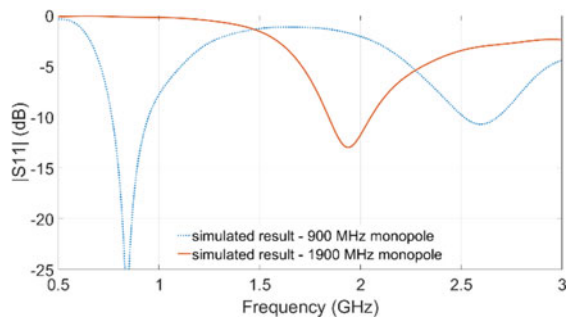


Fig. 6. Simulated S_{11} parameter magnitude for the quarter wavelength monopole antenna.

Fig. 4. According to [27], calculation of the effective permittivity for a quarter wavelength monopole is approximated by:

$$\epsilon_{eff} = \frac{\epsilon_r + 1}{2} + \frac{\epsilon_r - 1}{2} \times \left[\frac{1}{\sqrt{1 + (12 \times h/W_a)}} + 0.04 \times \left(1 - \frac{W_a}{2} \right) \right], \quad (5)$$

where h is the thickness of the substrate; W_a is the trace width.

The initial design parameters are set as $L_1 + L_2 = \lambda_{eff}/4$, where λ_{eff} is the effective wavelength at 900 or 1900 MHz, given by $\lambda_{eff} = \lambda_0/\sqrt{\epsilon_{eff}}$, with λ_0 being the free space wavelength. After parametric analysis, the parameters were set to $L_1 = 25$ mm, $L_2 = 46.8$ mm, $W_a = 4$ mm for the monopole resonating at 900 MHz and $L_1 = 18$ mm, $L_2 = 15$ mm, $W_a = 3.35$ mm for the monopole resonating at 1900 MHz.

The next step in the design process is to include a full ground plane and a single AMC cell in the quarter wavelength monopole. The final design parameters were found after the optimization process. The resulting antenna layout is shown in an exploded view in Fig. 5. The final set of parameters are $L_1 = 26$ mm, $L_2 = 49$ mm, $S = 4$ mm for the monopole at 900 MHz and $L_1 = 24$ mm, $L_2 = 23$ mm, $S = 12$ mm for the monopole at 1900 MHz.

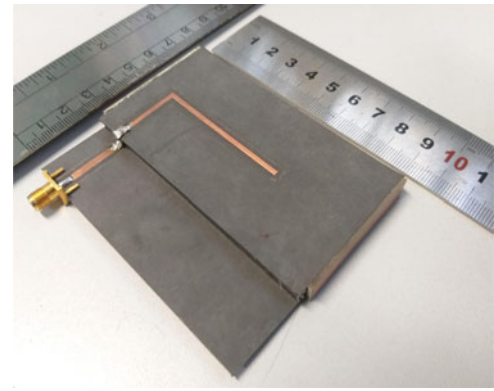


Fig. 7. A 900 MHz monopole on the AMC cell prototype picture.

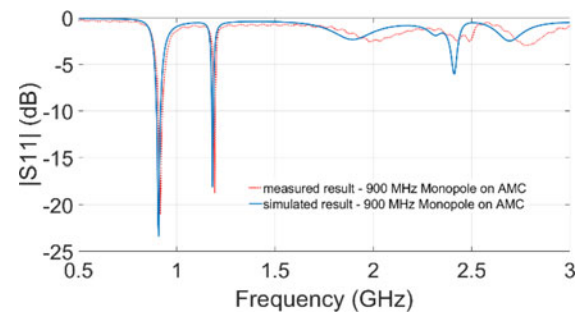


Fig. 8. Simulated and measured S_{11} parameter magnitude for the 900 MHz monopole antenna on the AMC cell.

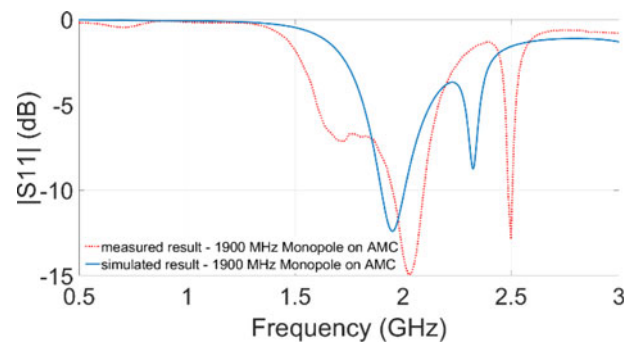


Fig. 9. Simulated and measured S_{11} parameter magnitude for the 1900 MHz monopole antenna on the AMC cell.

Results

The quarter wavelength bent monopoles, with and without AMC, were simulated using the CST Studio® software. The simulated S_{11} parameter magnitude (in dB) for the monopoles without AMC is shown in Fig. 6. The S_{11} result shows a resonance around 850 MHz and a -6 dB bandwidth of 335 MHz for the 900 MHz monopole and a resonance around 1950 MHz and a -6 dB bandwidth of 490 MHz for the 1900 MHz monopole. When including a full ground plane, this monopole is mismatched for all simulated frequencies.

The quarter wavelength monopoles on the AMC cell were prototyped and the S_{11} parameter was measured using Agilent Field Fox N9912a vector network analyzer. Figure 7 shows the 900

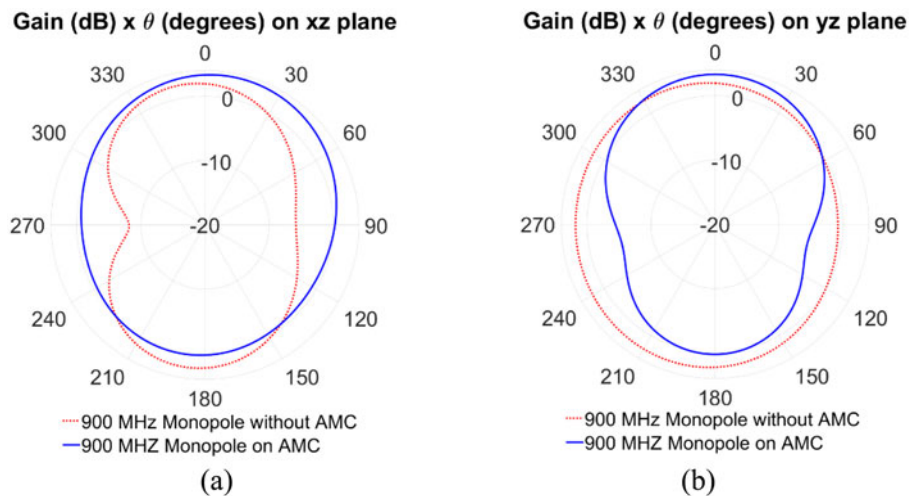


Fig. 10. Simulated elevation patterns for the 900 MHz quarter wavelength monopole without AMC and on AMC cell. (a) Gain on the xz plane. (b) Gain on the yz plane.

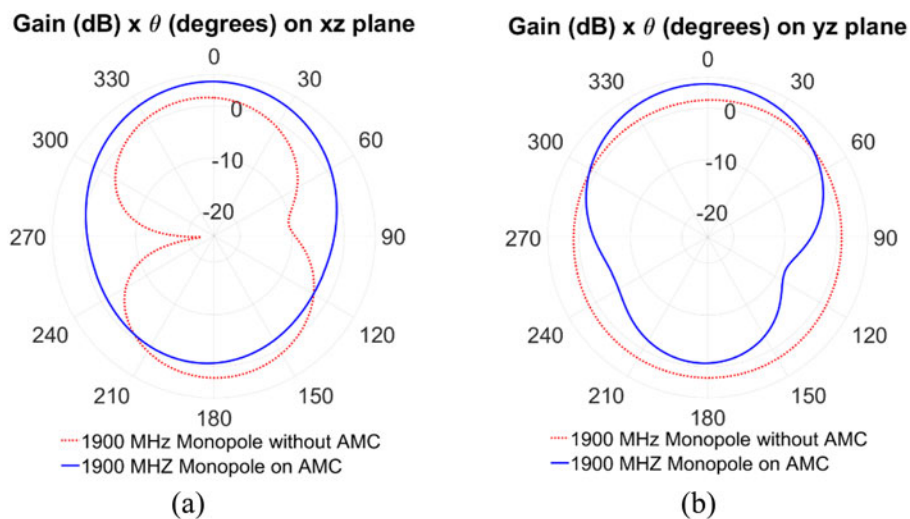


Fig. 11. Simulated elevation patterns for the 1900 MHz quarter wavelength monopole without AMC and on AMC cell. (a) Gain on the xz plane. (b) Gain on the yz plane.

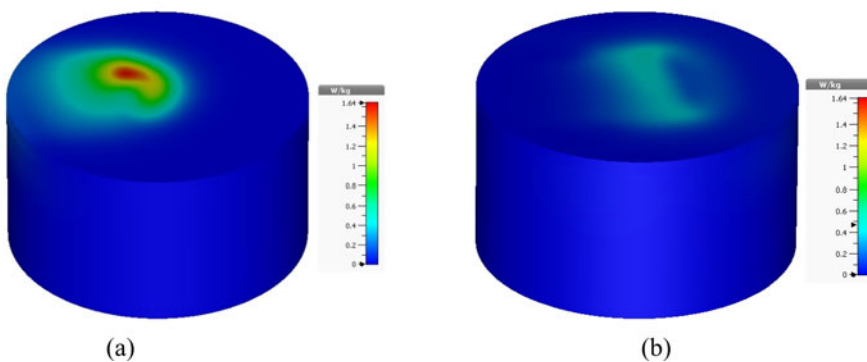


Fig. 12. Simulated SAR results of the 900 MHz quarter wavelength monopole (a) without AMC and (b) on AMC cell.

MHz monopole on AMC. The simulated and measured S_{11} parameter magnitudes (in dB) are shown in Fig. 8. Good agreement between simulation and measurement is obtained. The S_{11} results show a resonance close to 900 MHz and a -6 dB bandwidth of 37 MHz. Figure 9 shows the simulated and measured S_{11} parameter magnitude (in dB) for the 1900 MHz monopole on AMC. Some discrepancy between simulation and measurement was observed

despite repeated prototyping. This may be due to inaccuracies in the prototyping process and the high sensitivity of the S_{11} to the alignment between the AMC and the monopole. The S_{11} results show a resonance close to 1950 MHz and a -6 dB bandwidth of 250 MHz.

Simulated gain radiation pattern in elevation planes is shown in Figs 10 and 11, for the antennas. These results show a nearly

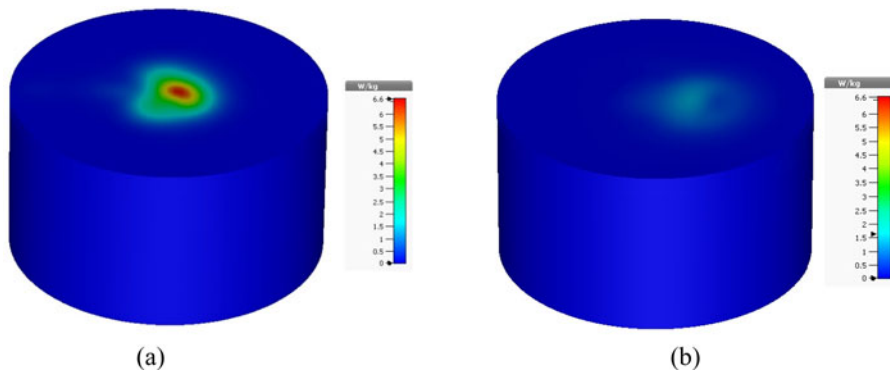


Fig. 13. Simulated SAR results of the 1900 MHz quarter wavelength monopole (a) without AMC and (b) on AMC cell.

omnidirectional radiation pattern for the quarter wavelength monopoles without AMC cell. The maximum simulated gain and radiation efficiency for the 900 MHz monopole antenna without AMC are, respectively, 2.42 dB and 95%. For the 1900 MHz monopole without AMC, these are, respectively, 2.16 dB and 98%. The simulated gain radiation pattern results for the antennas on the AMC cell show a slightly more directive antenna in comparison to the quarter wavelength monopole antenna without AMC. The 900 MHz monopole antenna on AMC shows a 4.4 dB front-to-back ratio, 3.9 dB maximum gain, and 95% radiation efficiency. The 1900 MHz monopole antenna on AMC shows a 5.4 dB front-to-back ratio, 4.69 dB maximum gain, and 98% radiation efficiency.

The SAR was simulated for the four antennas at a distance of 6 mm from the phantom. In order to save computer time, a four-slab flat phantom [28] instead of anthropomorphic models was used to evaluate the SAR. This phantom is composed of four cylinder layers (3, 6, 6, and 100 mm thick) with the mean dielectric parameters of the skin, fat, skull, and brain tissues. Each antenna was fed with 250 mW accepted power.

The simulated SAR results for the 900 MHz antenna are shown in Fig. 12. The simulated 1 g ps SAR (peak spatial SAR over 1 g of tissue) for the 900 MHz antennas without and with AMC were 1.63 W/kg (slightly above the FCC [6] limit) and 0.466 W/kg, respectively. Then a reduction of around 70% was obtained when including the AMC. The simulated SAR results for the 1900 MHz antenna are shown in Fig. 13. The simulated 1 g ps SAR (peak spatial SAR over 1 g of tissue) for the 1900 MHz antennas without and with AMC were 6.6 and 1.61 W/kg, respectively. Then a reduction of around 75% was obtained when including the AMC.

Simulated results show a reduction of around 70% in the 1 g psSAR for the monopole antennas with the AMC in comparison to the monopole antenna without AMC. However, the -6 dB bandwidth when including the AMC is significantly reduced.

Since current mobile handset designs radiate nearly one-half of the emitted power into the user's head and while the short- and long-term biological implications of this are yet to be fully determined, the absorption by the user's head is expected to decrease the radiation efficiency by more than 3 dB [1–3]. When the antenna is shielded from the user, this radiation efficiency can then be greatly increased.

Therefore, not only this reduces any possible health hazards but it is advantageous from the technical point of view too, since more energy is employed for communication, improving its quality (due to the improvement of the radio link budget) and reducing the battery drain (due to the automatic level control

for the necessary emitted power), which in turn affects the weight of the phone too. This AMC layer also provides high EM surface impedance, then allowing the antenna to lie directly adjacent to the backplane without being shorted out. This allows compact antenna designs where the radiating elements are confined to limited spaces.

These antennas can also be adequate for applications in MIMO (Multiple Input Multiple Output) systems, such as in LTE, WLAN, and WiMax.

Discussion and conclusions

The design, simulations, and optimized results for a novel low SAR monopole antenna on a single AMC cell were described in this paper.

Simulated results show 1 g ps SAR reduction around 70 and 75%, respectively, at 900 and 1900 MHz for the monopole with the AMC in comparison to the monopole without AMC. Then, these antennas may be adequate to reduce the EMF absorbed in the user's head and body, improving therefore the quality of communication, reducing the battery drain, and reducing the user's health risks.

Acknowledgement. Part of this work was supported by Dr. Paul Héroux from McGill University, Canada.

References

1. de Salles AA, Bulla G and Rodriguez CEF (2006) Electromagnetic absorption in the heads of adults and children due to mobile phone operation close to the head. *Electromagnetic Biology and Medicine* 25, 349–360.
2. Gandhi OP, Lazzi G and Furse CM (1996) Electromagnetic absorption in the human head and neck for mobile telephones at 835 and 1900 MHz. *IEEE Transactions on Microwave Theory and Techniques* 44, 1884–1897.
3. Gandhi OP, Morgan LL, de Salles AA, Han YY, Herberman RB and Davis DL (2012) Exposure limits: the underestimation of absorbed cell phone radiation, especially in children. *Electromagnetic Biology and Medicine* 31, 34–51.
4. International Commission on Non-Ionizing Radiation Protection (ICNIRP) (1998) Guidelines for limiting exposure to time-varying electric, magnetic and electromagnetic fields (up to 300 GHz), international commission on non-ionizing radiation protection. *Health Physics* 74, 494–522.
5. IEEE standard for safety levels with respect to human exposure to radio frequency electromagnetic fields, 3 kHz to 300 GHz, IEEE Standard C95.1-1991, 2005.
6. Federal Communications Committee (FCC) and Office of Engineering and Technology (2001) Evaluating compliance with FCC guidelines for human exposure to radiofrequency electromagnetic fields, additional

- information for evaluating compliance of mobile and portable devices with FCC limits for human exposure to radiofrequency emissions. Supplement C (Ed. 01-01) to OET Bulletin 65 (Ed. 97-01).
7. **Agence Nationale des Fréquences** (2018) ANFR webpage [Online] Available at <http://data.anfr.fr/explore/dataset/dastelephonimobile/?disjunctive.marque&disjunctive.modele&sort=marque>.
 8. **Hardell L and Carlberg M** (2015) Mobile phone and cordless phone use and the risk for glioma – analysis of pooled case-control studies in Sweden, 1997–2003 and 2007–2009. *Pathophysiology* **22**, 1–13.
 9. **INTERPHONE Study Group** (2010) Brain tumour risk in relation to mobile telephone use: results of the INTERPHONE international case-control study. *International Journal of Epidemiology* **39**, 675–694.
 10. **Coureau G, Bouvier G, Lebailly P, Fabbro-Peray P, Gruber A, Leffondre K, Guillamo JS, Loiseau H, Mathoulin-Pélissier S, Salamon R and Baldi I** (2014) Mobile phone use and brain tumours in the CERENAT case-control study. *Occupational and Environmental Medicine* **71**, 514–522.
 11. **Sadetzki S, Chetrit A, Jarus-Hakak A, Cardis E, Deutch Y, Duvdevani S, Zultan A, Novikov I, Freedman L and Wolf M** (2008) Cellular phone use and risk of benign and malignant parotid gland tumours – a nationwide case-control study. *American Journal of Epidemiology* **167**, 457–467.
 12. **WHO/IARC Working Group** (2011) Carcinogenicity of radiofrequency electromagnetic fields. *The Lancet Oncology* **12**, 624–626.
 13. **IARC (International Agency for Research on Cancer)** (2013) IARC monographs on the evaluation of carcinogenic risks to humans. In: Non-ionization Radiation, Part 2: Radiofrequency Electromagnetic Fields, vol. 102. IARC Press, Lyon, France, p. 406.
 14. **Bankro M** (2016) *Investigation of Mobile Phone SAR Reduction* (Dr. Ing. dissertation). Universität Duisburg-Essen, URN: urn:nbn:de:hbz:464-20160830-080459-5 DuEPublico ID: 41990; Library shelfmark YDA2032.
 15. **Laila D, Sujith R, Nair SM, Aanandan CK, Vasudevan K and Mohanan P** (2011) Modified CPW fed monopole antenna with a radiation pattern suitable for mobile handset. International Conference on Communications and Signal Processing, pp. 370–373.
 16. **Wei Y and Roblin C** (2012) Multislot antenna with a screening backplane for UWB WBAN applications. *International Journal of Antennas and Propagation* **2012**, 1–12.
 17. **Ma KP, Hirose K, Yang FR, Qian Y and Itoh T** (1998) Realization of magnetic conducting surface using novel photonic bandgap structure. *Electronics Letters* **34**, 2041–2042.
 18. **Goussetis G, Feresidis A and Vardaxoglou J** (2006) Tailoring the AMC and EBG characteristic of periodic metallic arrays printed on grounded dielectric substrate. *IEEE Transactions on Antennas and Propagation* **54**, 82–89.
 19. **Yang F and Rahmat-Samii Y** (2003) Reflection phase characterizations of the EBG ground plane for low profile wire antenna applications. *IEEE Transactions on Antennas and Propagation* **51**, 2691–2703.
 20. **Kamardin K, Rahim MKA, Hall PS, Samsuri NA, Jalil ME and Ayop O** (2013) Textile artificial magnetic conductor waveguide sheet with monopole antennas for body centric communication. *7th Eur. Conf. on Antennas and Propagation (EuCAP)*, pp. 366–370.
 21. **Broas R, Sivenpiper D and Yablonoitch E** (2001) A high-impedance ground plane applied to a cellphone handset geometry. *IEEE Transactions on Microwave Theory and Techniques* **49**, 1262–1265.
 22. **Hwang JN and Chen FC** (2006) Reduction of the peak SAR in the human head with metamaterials. *IEEE Transactions on Antennas and Propagation* **54**, 3763–3770.
 23. **Kwak SI, Sim DU, Kwon JH and Choi HD** (2008) Experimental tests of SAR reduction on mobile phone using EBG structures. *Electronics Letters* **44**, 568–569.
 24. **Raad H, Abbosh A, Al-Rizzo H and Rucker D** (2013) Flexible and compact AMC based antenna for telemedicine application. *IEEE Transactions on Antennas and Propagation* **61**, 524–531.
 25. **Kwak SI, Sim DU, Kwon JH and Yoon YJ** (2017) Design of PIFA with metamaterials for body-SAR reduction in wearable applications. *IEEE Transactions on Electromagnetic Compatibility* **59**, 297–300.
 26. **Yang F and Rahmat-Samii Y** (2009) Electromagnetic band gap structures in antenna engineering [ref. Electromagnetic Band Gap Structures in Antenna Engineering, Cambridge University Press, Cambridge].
 27. **Rushingabigwi G and Sun L** (2015) Design of an 868 MHz printed S-shape monopole antenna. *Journal of Computer and Communications* **3**, 49–55.
 28. **Fernández-Rodríguez C, de Salles AA and Davis DL** (2015) Dosimetric simulations of brain absorption of mobile phone radiation – the relationship between psSAR and age. *IEEE Access* **3**, 2425–2430.



Giovanni Bulla received a degree in physics in 2004 and his Ph.D. degree in Electrical Engineering in 2010 from the Federal University of Rio Grande do Sul – UFRGS, Porto Alegre, Brazil where he serves as an assistant professor since 2016. His research interests include electromagnetic simulation, EMI/EMC, antenna design, RFID and biological effects of RF.



Alvaro Augusto A. de Salles was born on 6 March 1946 in Bagé, Rio Grande do Sul, Brazil. He earned the B.Sc. degree in Electrical Engineering from Escola de Engenharia, Universidade Federal do Rio Grande do Sul – UFRGS, Porto Alegre, Brazil in 1968, the M.Sc. degree in Electrical Engineering from Pontifícia Universidade Católica do Rio de Janeiro PUC/RJ, Rio de Janeiro in 1970, and the Ph.D. degree in Electrical Engineering from the University of London, London, 1978–1982. He was an Associate Professor at the PUC/RJ from 1970 to 1991. Since 1991 to the present, he has been a Professor at UFRGS. His main research interests are microwave semiconductor devices, optoelectronic devices, mobile communications, antennas, and biological effects of non-ionizing radiation. Dr. de Salles has published more than 80 papers in international conferences and magazines.



Claudio Enrique Fernandez Rodriguez is an Associate Professor at the Federal Institute of Education, Science and Technology of Rio Grande do Sul – IFRS, in Canoas, Brazil. He received his B.Sc. degree from the State University of Campinas – UNICAMP, Campinas, Brazil in 1996, and his M.Sc. degree from the Federal University of Rio Grande do Sul – UFRGS, Porto Alegre, Brazil in 2000, both in Electrical Engineering. He coordinates a UN Development Program for the Strengthening of the Technological Education in Brazil and in Uruguay through the creation of binational schools and was the founding Dean of the Electrical Engineering School at the Federal Center of Technological Education of Pelotas – CEFET-RS, Pelotas, Brazil. He served as a Director of Public Outreach of IRFS/Canoas and as a Labour Union state secretary. His research interests include the biological effects of microwaves and RF, numerical methods in computational electromagnetism and engineering education. He is the co-author of over 60 technical publications and a book chapter and served as a reviewer of several international publications.